RSC Advances

ROYAL SOCIETY OF CHEMISTRY

www.rsc.org/advances

Ordered Exfoliated Silicate Platelets Architecture: Hydrogen Bonded Poly(acrylic acid)-Poly(ethylene oxide)/Na-Montmorillonite Complex Nanofibrous Membranes Prepared by Electrospining Technique

Zahed Shami[1,*], Naser Sharifi-Sanjani[1,*], Bafrin Khanyghma[2], Sadegh Farjpour[3], Azam Fotouhi[1]

[1]Polymer Laboratory, Chemistry Department, School of Science, University of Tehran, Tehran, Iran

[2]Organic Laboratory, Chemistry Department, School of Science, University of Tehran, Tehran, Iran

[3]Kharazmi Technology Development, Supplying Petrochemical Industries Parts Equipment &Chemical Engineering CO (SPEC), Tehran, Iran

Corresponding authors

*E-mail: zahed.shami@ut.ac.ir; zahed.shami@gmail.com, and nsanjani@khayam.ut.ac.ir

Abstract

Hydrogen bonded Poly(acrylic acid)-poly(ethylene oxide) interpolymer nanofibrous membranes containing the well-arranged/dispersed exfoliated Na-montmorillonite platelets obtained successfully by the electrospinning technique. The as-spun composite nanostructures were characterized by X-ray diffraction patterns and electron microscopy, confirm the formation of a favoring ordered exfoliated architecture along the fiber axis. Thermal analysis suggested that increase in both the thermal stability and melting point of the as-synthesized composite nanostructures could be a result of ordered exfoliated morphology as well as the well-distributed clay platelets along the fiber axis. Improved morphological and thermal properties assigned to aligned clay platelets induced by the electrospinning technique make the as-spun non-woven

membranes as a more promising candidate in such tissue engineering, drug delivery, fuel cell proton exchange membranes and environmental pollution treatment applications.

Keywords: Electrospinning, composite membrane, poly(acrylic acid), poly(ethylene oxide), Na-montmorillonite

1. Introduction

The unique medical and industrial characterizations of the clay layered silicate/polymer nanocomposites have been caused to attract much attention of nanoscience studies in both the experimental and commercial scales, indicating high stiffness, highly thermal stability, better barrier properties as well as biocompatibility even with a small amount of silicate[1-4]. However, the alignment of the well-dispersed clay platelets in the polymer matrix (intercalation/exfoliation) as well as the interaction between the polymer matrix and clay surface have been a challenge to synthesize the polymer/layered silicate nanocomposites with improved properties. Unlike the conventional techniques that is needed to the additional agents, the electrospinning process is an effective technique for the preparation of layered silicate/polymer composite nanofibers with a highly dispersion/orientation of the clay layered nanomaterials as well as a controllable morphology, especially the exfoliated silicate layers morphology[5-9]. Exfoliation has been an ultimate goal of most researchers in this area because this morphology is expected to lead to dramatic improvement of the properties with a reduced loading of fillers compared with traditional composites[10, 11]. The overall morphology of electrospun clay nanocomposites is very complex, where in the range of exfoliated structures, a classification of ordered, partially ordered and disordered ones was introduced to adequately describe nanoscale morphology and to avoid confusion in the structure-properties relationship of nanocomposites[12]. Silvestre and et al[13] proposed an expanded classification scheme where the intercalated and

exfoliated structures can be listed in the ordered or disordered structures (Figure 1a), depending on the change of spacing and orientation of nanoplatelets. It is found that the large shear forces induced by the electric field on the fibers as well as their rapid solidification resulted from the bending and whipping instability could result in a high chain orientation along the direction of the fiber axis as well as alignment of anisotropic layered nanofillers in the polymer matrix, mostly leading to the formation of a favored exfoliated silicate architecture[14-18]. There are many reports for the synthesis of electrospun clay layered silicate/polymer composite nanofibers including one or multi-type polymers[19-24]. Nevertheless, to the best of our knowledge, there are not any reports about electrospun Poly(acrylic acid)-poly(ethylene oxide) (PAA-PEO) interpolymer complex composites containing the clay layered silicate nanoplatelets. In previous study, we present a novel approach to prepare hydrogen bonded PAA-PEO interpolymer complex nanofibrous membranes with unique characterization[25]. Herein, we for the first time synthesized a well-designed electorspun hydrogen bonded poly(acrylic acid)-poly(ethylene oxide) composite nanofibrous membranes containing Na-montmorillonite (Na-MMT) (Figure 1b), suggesting to be benefit in exchange-proton membranes in fuel cells, tissue engineering, drug delivery and wastewater treatment which can be attributed to easy availability of functional groups, high specific surface area, the well-arranged pores as well as superior specifications of two-dimensional clay layered nanoplatletes such as enhanced thermal, mechanical and barrier properties along with their biocompatibility [26-39]. The as-synthesized composite fibers were investigated by X-ray diffraction (XRD), scanning electron microscopy (SEM), transmission electron microscopy (TEM), termogravimetric (TGA) and differential scanning calorimetric (DSC) analysis.

2. Experimental

2.1. Materials

The polymeric constituents of the samples are poly(acrylic acid) (Mw= 240,000 gr/mol, Aldrich) and poly(ethylene oxide) (Mw= 600,000 gr/mol, Across organic). 1.0 M NaOH standard solution (Merck) was used as pH regulator. Na-montmorillonite is layered clay, obtained from Southern Clay Products, USA. Distilled water was used as a solvent.

2.2. Preparation of hydrogen bonded PAA-PEO/Na-montmorillonite interpolymer composite solutions

At first, the appropriate amounts of the clay nanofiller were dispersed into 10.0 mL distilled water for 6 h under the magnetic stirring at room temperature. To promote swelling and dispersing, the clay nanomaterials dispersed in distilled water, was sonicated for 30 minutes using an ultrasonic generator equipped with an ice water bath. PEO powder (0.53 gr) was added to each of these dispersions and magnetically stirred at 50.0˚C for 12 h to obtain 5.0 wt.% PEO homogeneous solutions containing 1.0, 2.0 and 4.0 wt.% Na-montmorillonite. Then 5.0 wt.% PAA aqueous solution was dropwise added to each of the above-mentioned dispersions and magnetically stirred at 50.0 °C for other 6 h to obtain PAA-PEO/Na-montmorillonite composites with the weight ratio of 1:1 of PAA/PEO containing 1.0, 2.0 and 4.0 wt.% of Na-montmorillonite. The pH of the solutions was regulated for a value of 5.3 using 1.0 M NaOH standard solution.

2.3. Electrospinning of the as-synthesized composite solutions

The electrospinning experiments were performed under ambient conditions at 25.0 ˚C and 47.0% relative humidity. The polymer solution was placed into a 10.0 mL plastic syringe with a steel needle having an inner diameter of 1.0 mm (18 gauges). A clamp connected the high-voltage

power supply (MH 100 series, HiTek Power Co., UK) to the needle. A piece of aluminum foil placed at 17.5 cm directly facing the needle, act as a grounded collector. The applied voltage and feed rate of the solution were fixed at 17.0 kV and 0.7 mL/h, respectively.

2.4. Characterization

The morphology of the as-spun composite fibers was observed under a SEM (ZEISS DSM 960A, 20.0 kV) at an accelerating voltage of 10.0 kV. Prior to scanning under SEM, the samples were sputter-coated for 100 S with gold, using a BALZERS SCD 004 fine coater (Germany). The clay layered silicate architecture was investigated by means of TEM, using a CEM 902A ZEISS, (Germany) with an 80.0 keV accelerating voltage. XRD analysis was performed at room temperature in the reflection mode on a Philips X-ray diffractometer with Cu K radiation of a wavelength of 1.54056Aº. A scanning rate of 2˚/min was used. DSC (DSC Q100, TA) thermograms were analyzed in the temperature range of -50 to 300 °C at a heating rate of 10º/min. A TA Instruments Q50 TGA was used for TGA analysis. The samples were heated from the room temperature up to 600 ºC at a heating rate of 10˚/min in argon atmosphere.

3. Results and discussion

3.1. X-ray Diffraction

The spacing between the clay platelets or gallery spacing is an indicator of the extent of the intercalation/exfoliation of clay platelets within a polymer matrix and could be observed by using XRD. Generally, intense reflection in the range of 3-9° (2θ) indicates an ordered intercalated architecture. On the other hand, exfoliated morphology, where single silicate layers are homogeneously dispersed into the polymer matrix and XRD patterns with no distinct diffraction peak in the range of 3-9° (2θ) could be observed. The XRD patterns of Na-montmorillonite and its composite nanofibers are shown in Figure 2. The pristine Na-

montmorillonite exhibited a broad diffraction peak at 2θ = 6.61-9.65°. The XRD pattern of hydrogen bonded PAA-PEO/Na-MMT composite nanofibrous membranes, however, did not show the diffraction peak in XRD patterns. Obviously, these observations confirm the formation of exfoliated Na-MMT layers within PAA-PEO fibers.

3.2. Transmission Electron Microscopy Analysis

TEM analysis is complementary to XRD and can give insights into the spatial distribution of the layers. The exfoliated state is confirmed by TEM analysis as shown in Figure 3[40, 41]. TEM images of the as-spun composite nanofibrous membranes containing 1.0 (a), 2.0 (b) and 4.0 wt.% Na-MMT (c) are revealed in Figure 3 (The dark lines represent an individual clay layer, whereas the bright area represents the PAA-PEO fiber matrix). TEM images reveal that the majority of the Na-MMT platelets have ordered exfoliated morphology and they were the well-distributed within the fiber matrix, and oriented along the fiber axis. However, these images indicated that some multilayer stacks of nanoplatelets could be observed within the nanofibers. This clearly indicates the feasibility of electrospinning technique for the controllable preparation of two-dimensional ordered exfoliated platelets architecture with a desired alignment of these platelets along the direction of the fiber axis, which is the critical for the conventional techniques in preparation of such type morphology. In the present study it is proposed that the strong elongation forces imposed on the PAA-PEO/Na-MMT Taylor cone during the electrospinning process will forced the clay platelets to be oriented in the direction of the fiber axis, which causes platelets to mostly show the well-ordered exfoliation morphology[42].

3.3. Scanning Electron Microscopy Analysis

Figure 4 reveals the SEM images of pure PAA-PEO nanofibers (a) and PAA-PEO/Na-MMT composite nanofibers containing 1.0 (b), 2.0 (c) and 4.0 wt.% Na-MMT (d). The nanofibers were

randomly distributed to form the three-dimensional fibrous membranes. The morphology and average diameter of the as-spun nanocomposite fibers were significantly affected by the loadings of Na-MMT as is observed in Figure 4. By carefully comparing the SEM images, it can be observed the presence of continued uniform small clay agglomerations within whole electrospun nanofibers (marked with the dash yellow circles). Such the well-dispersed agglomerations is enhanced with increase in the clay amount from 1.0 to 4.0 wt.% , conform the well dispersed clay nanomaterials even in the high amounts of clay nanofillers (Figure 4d). Furthermore, in agreement with TEM images the presence of some aggregations marked with the dash red circles confirm the formation of some multilayer stacks.

3.4. Thermogravimetric Analysis

Thermogravimetric analysis was conducted to investigate thermal stability of the as-prepared nanofibers. Figure 5 shows the plots of weight variation versus temperature and the first derivative of the corresponding TGA scan (DTGA) for the clay-containing nanofibers of PAA-PEO with amounts of 0.0, 1.0, 2.0, and 4.0 wt. % of Na-MMT. As was presented in previous study[25], the investigation of the thermal behavior of PAA-PEO complex (1:1 w/w) indicates that two main reaction stages take place during the thermal degradation of PAA and PEO complex in argon atmosphere. The first stage of the thermal degradation in pure PAA-PEO (1:1 w/w) nanofibers was at around 177.2 ºC corresponded to the breaking of chemical bonds along with the formation of cyclic structures (glutaric anhydride)[25, 43]. Next step, the thermal degradation started about 341.0 ºC, is related to the destruction of carboxylic groups and CO_2 elevation as well as main chain scission. The thermal behavior of PAA-PEO/Na-MMT composites nanofibers containing 1.0 and 2.0 wt.% clay platelets was nearly similar to those of Pure PAA-PEO nanofibers and the thermal degradation is started about 176.3 and 183.2 °C, respectively.

Nevertheless, the as-spun composite nanofibers with 4.0 wt. % Na- MMT exhibited the different degradation behavior, where degradation in the first stage takes place at higher temperature (about 197.7 °C). Furthermore, in compared with PAA-PEO/Na-MMT containing 0.0, 1.0 and 2.0 wt.% Na-MMT that revealed the residual weight about 14.7, 17.1 and 17.9 % at 500 °C, respectively, the residual weight in the PAA-PEO/Na-MMT is about 30.2 %. Enhanced thermal stability in the composite nanofibers, especially in PAA-PEO/Na-MMT with 4.0 wt.% clay is suggested to be result of a well dispersion/orientation of exfoliated platelets induced by high tension forces in electrospinning process.

3.5. Differential Scanning Calorimetric Analysis

The melting point of PAA-PEO/Na-MMT nanofibers were investigated by DSC, as is observed in Figure 6. Pure PAA-PEO fibers showed a peak of melting transition at 53.8 °C. This peak shifted to 63.8, 63.3 and 59.9 °C for PAA-PEO/Na-MMT composite nanofibrous membranes with 1.0, 2.0 and 4.0 wt.% MMT, respectively. Improvement in the melting temperature of the as-spun composite fibers suggest be owing to the well-arranged polymer chains and clay platelets by the electric field.

4. Conclusions

Well-dispersed/oriented exfoliated silicate platelets aligned in the direction of the fiber axis obtained successfully by electrospinning. SEM images shown the well-distributed clay nanomaterials into electrospun fiber composites even at 4.0 wt.% Na-montmorillonite concentration. TEM images as well as XRD patterns confirmed the well-dispersed/oriented exfoliated clay platelets. The as-spun PAA-PEO/Na-MMT composite nanostructures exhibited improved thermal properties assigned to uniformity in morphology that could be useful applicably.

Acknowledgements

This study was supported by Kharazmi Technology Development (SPEC). The authors would like to thank especially Ms. Barbora Ehrlichová for proofreading.

Abbreviations

C [°C] Celsius Temperature

D [nm] fiber thickness/diameter

d [cm] distance

H [h] time

M [mol/L] molarity

Mw [gr/mol] molecular weight average

R [mL/h] injection rate

S [s] time

t [min] time

V [mL] volume of solution

Wt [gr or mg] weight percent

ΔE [kV] applied voltage

ΔV [keV] accelerator volatge

λ [Aº] diffraction angle

θ [°] wavelength of X-ray diffraction

References

1. L. Chen and Y.-Z. Wang, *Polymers for Advanced Technologies*, 2010, **21**, 1-26.

2. S. S. Ray, *Clay-Containing Polymer Nanocomposites: From Fundamentals to Real Applications*, Elsevier Science, 2013.

3. H. Lu, L. Song and Y. Hu, *Polymers for Advanced Technologies*, 2011, **22**, 379-394.

4. T Richard Hull and B. K. Kandola, in *Fire Retardancy of Polymers: New Strategies and Mechanisms* RCS, 1 edn., 2009, p. 456.

5. Y. Cai, N. Wu, Q. Wei, K. Zhang, Q. Xu, W. Gao, L. Song and Y. Hu, *Surface and Coatings Technology*, 2008, **203**, 264-270.

6. L. Wang, Y.-B. Yan, Q.-Q. Yang, J. Yu and Z.-X. Guo, *Journal of Materials Science*, 2012, **47**, 1702-1709.

7. M. Nouri, J. Mokhtari and M. Rostamloo, *Fibers and Polymers*, 2013, **14**, 957-964.

8. W. Liu, S. Yee and S. Adanur, *The Journal of The Textile Institute*, 2013, 1-7.

9. Y. Wang, M. Li, J. Rong, G. Nie, J. Qiao, H. Wang, D. Wu, Z. Su, Z. Niu and Y. Huang, *Colloid and Polymer Science*, 2013, **291**, 1541-1546.

10. K. Wang, L. Chen, J. Wu, M. L. Toh, C. He and A. F. Yee, *Macromolecules*, 2005, **38**, 788-800.

11. H. Dalir, R. D. Farahani, V. Nhim, B. Samson, M. Lévesque and D. Therriault, *Langmuir*, 2011, **28**, 791-803.

12. R. Kotsilkova and P. Pissis, *Thermoset Nanocomposites for Engineering Applications*, Smithers Rapra Technology, 2007.

13. Clara Silvestre, Sossio Cimmino, Donatella Duraccio and R. Kotsilkova, in *Thermoset Nanocomposites for Engineering applications*, ed. K. Rumiana, Smithers Rapra Technology, 2007.

14. S. Vivekanandhan, M. Schreiber, A. Mohanty and M. Misra, in *Handbook of Polymernanocomposites. Processing, Performance and Application*, eds. J. K. Pandey,

K. R. Reddy, A. K. Mohanty and M. Misra, Springer Berlin Heidelberg, 2014, pp. 361-388.

15. S. Torres-Giner and J. M. Lagaron, *Journal of Applied Polymer Science*, 2010, **118**, 778-789.

16. C. A. G. Beatrice, C. R. d. Santos, M. C. Branciforti and R. E. S. Bretas, *Materials Research*, 2012, **15**, 611-621.

17. N. Bitinis, M. Hernandez, R. Verdejo, J. M. Kenny and M. A. Lopez-Manchado, *Advanced Materials*, 2011, **23**, 5229-5236.

18. S. Pandey, M. G. H. Zaidib and S. K. Gururani, *Recent Developments in Clay- Polymer Nano Composites*, 2013.

19. M. S. Islam, J. H. Yeum and A. K. Das, *Journal of Colloid and Interface Science*, 2012, **368**, 273-281.

20. Z. Shami and N. Sharifi-Sanjani, *Fibers and Polymers*, 2010, **11**, 695-699.

21. M. Wang, J. H. Yu, A. J. Hsieh and G. C. Rutledge, *Polymer*, 2010, **51**, 6295-6302.

22. R. Neppalli, S. Wanjale, M. Birajdar and V. Causin, *European Polymer Journal*, 2013, **49**, 90-99.

23. B. S. Lalia, E. Guillen-Burrieza, H. A. Arafat and R. Hashaikeh, *Journal of Membrane Science*, 2013, **428**, 104-115.

24. L. Yu and P. Cebe, *Polymer*, 2009, **50**, 2133-2141.

25. Z. Shami and N. Sharifi-Sanjani, *International Polymer Processing*, 2011, **26**, 361-367.

26. D. S. Liu, J. N. Ashcraft, M. M. Mannarino, M. N. Silberstein, A. A. Argun, G. C. Rutledge, M. C. Boyce and P. T. Hammond, *Advanced Functional Materials*, 2013, **23**, 3087-3095.

27. T. R. Farhat and P. T. Hammond, *Advanced Functional Materials*, 2005, **15**, 945-954.

28. Z. Dong, S. J. Kennedy and Y. Wu, *Journal of Power Sources*, 2011, **196**, 4886-4904.

29. J. Choi, Case Western Reserve University, 2010.

30. J. Choi, R. Wycisk, W. Zhang, P. N. Pintauro, K. M. Lee and P. T. Mather, *ChemSusChem*, 2010, **3**, 1245-1248.

31. S. Mollá and V. Compañ, *Journal of Membrane Science*, 2011, **372**, 191-200.

32. I. Shabani, M. M. Hasani-Sadrabadi, V. Haddadi-Asl and M. Soleimani, *Journal of Membrane Science*, 2011, **368**, 233-240.

33. J. D. Snyder and Y. A. Elabd, *Journal of Power Sources*, 2009, **186**, 385-392.

34. W. G. Jang, J. Hou and H. s. Byun, *Desalination and Water Treatment*, 2011, **34**, 315-320.

35. N. Shubha, R. Prasanth, H. H. Hoon and M. Srinivasan, *Materials Research Bulletin*, 2013, **48**, 526-537.

36. P. Wang, J. Liu and T. Zhang, *Journal of Nanomaterials*, 2013, **2013**, 8.

37. B. Sarmento and J. das Neves, *Chitosan-Based Systems for Biopharmaceuticals: Delivery, Targeting and Polymer Therapeutics*, Wiley, 2012.

38. Z. Chen, X. Mo, C. He and H. Wang, *Carbohydrate Polymers*, 2008, **72**, 410-418.

39. J. Raghava Rao and B. U. Nair, *Bioresource Technology*, 2011, **102**, 872-878.

40. A. B. Morgan and J. W. Gilman, *Journal of Applied Polymer Science*, 2003, **87**, 1329-1338.

41. J. H. Hong, E. H. Jeong, H. S. Lee, D. H. Baik, S. W. Seo and J. H. Youk, *Journal of Polymer Science Part B: Polymer Physics*, 2005, **43**, 3171-3177.

42. M. R. Karim, H. W. Lee, R. Kim, B. C. Ji, J. W. Cho, T. W. Son, W. Oh and J. H. Yeum, *Carbohydrate Polymers*, 2009, **78**, 336-342.

43. L. Li and Y.-L. Hsieh, *Polymer*, 2005, **46**, 5133-5139.

Figure captions

Figure 1. (a) Classification of silica layered morphology into the polymer matrix, (b) Schematic illustration of process

Figure 2. XRD patterns of Na-MMT and PAA-PEO/Na-MMT nanocomposite fibers with 1.0, 2.0 and 4.0 wt.% Na-MMT

Figure 3. TEM images of PAA-PEO/Na-MMT nanocomposite fibes with 1.0 (a), 2.0 (b), and 4.0 wt.% Na-MMT (c)

Figure 4. SEM images of PAA-PEO/Na-MMT nanocomposite fibes with 0.0 (a), 1.0 (b), 2.0 (c), and 4.0 wt.% Na-MMT (d)

Figure 5. TGA (a) and DTGA (b) curves of pure PAA-PEO nanofibers and PAA-PEO/Na-MMT nanocomposite fibers

Figure 6. DSC curves of PAA-PEO nanofibers and PAA-PEO/Na-MMT nanocomposite fibers

Graphical Abstract (TOC)

The well-ordered/dispersed exfoliated clay platelets aligned along the as-electrospun PAA-PEO/Na-montmorillonite composite nanofibrous membranes successfully were synthesized for the first time

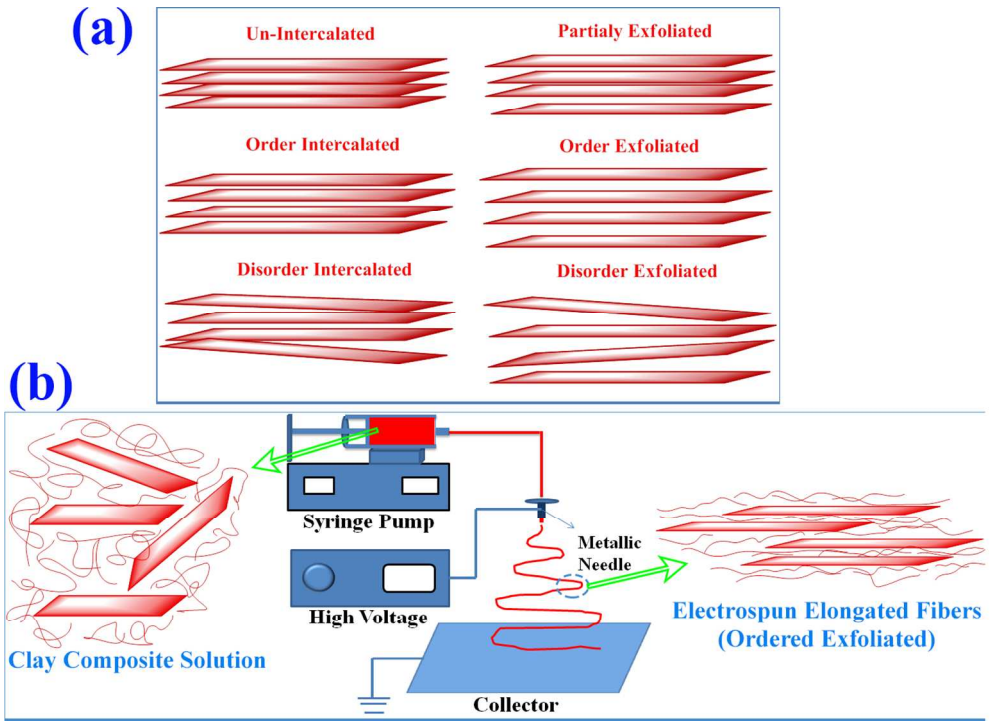

Figure 1. (a) Classification of silica layered morphology into the polymer matrix, (b) Schematic illustration of process
520x370mm (72 x 72 DPI)

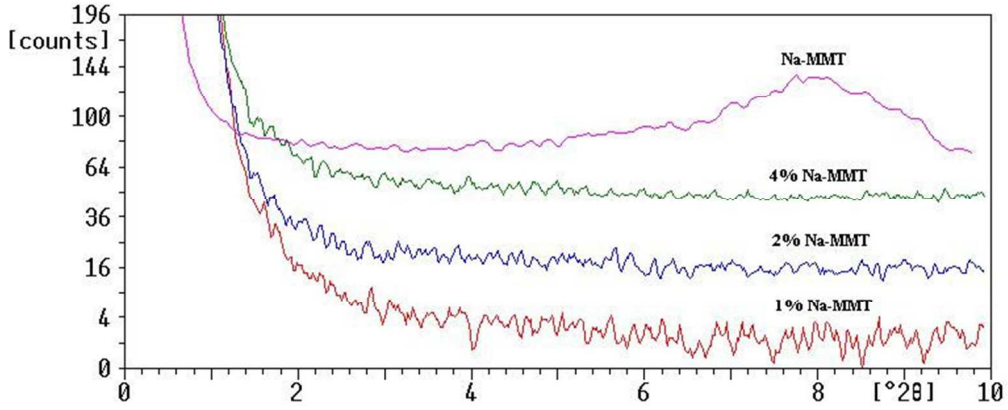

Figure 2. XRD patterns of Na-MMT and PAA-PEO/Na-MMT nanocomposite fibers with 1.0, 2.0 and 4.0 wt.% Na-MMT
201x83mm (96 x 96 DPI)

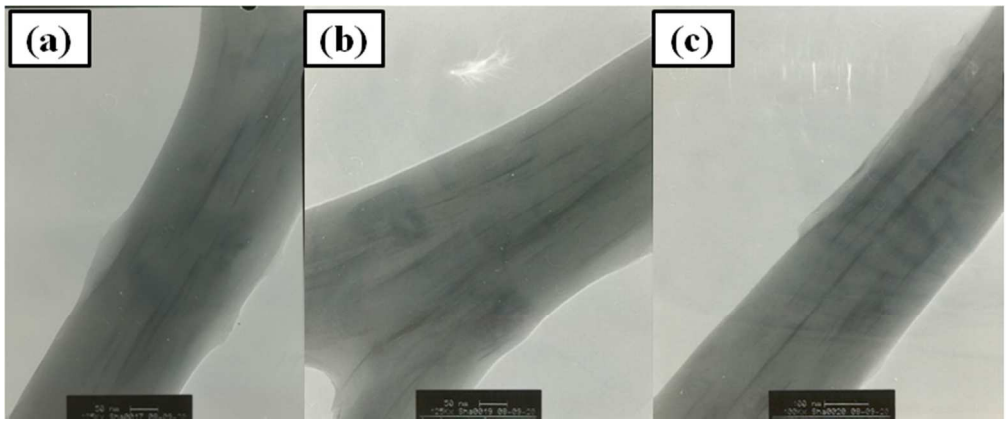

Figure 3. TEM images of PAA-PEO/Na-MMT nanocomposite fibes with 1.0 (a), 2.0 (b), and 4.0 wt.% Na-MMT (c)
217x89mm (96 x 96 DPI)

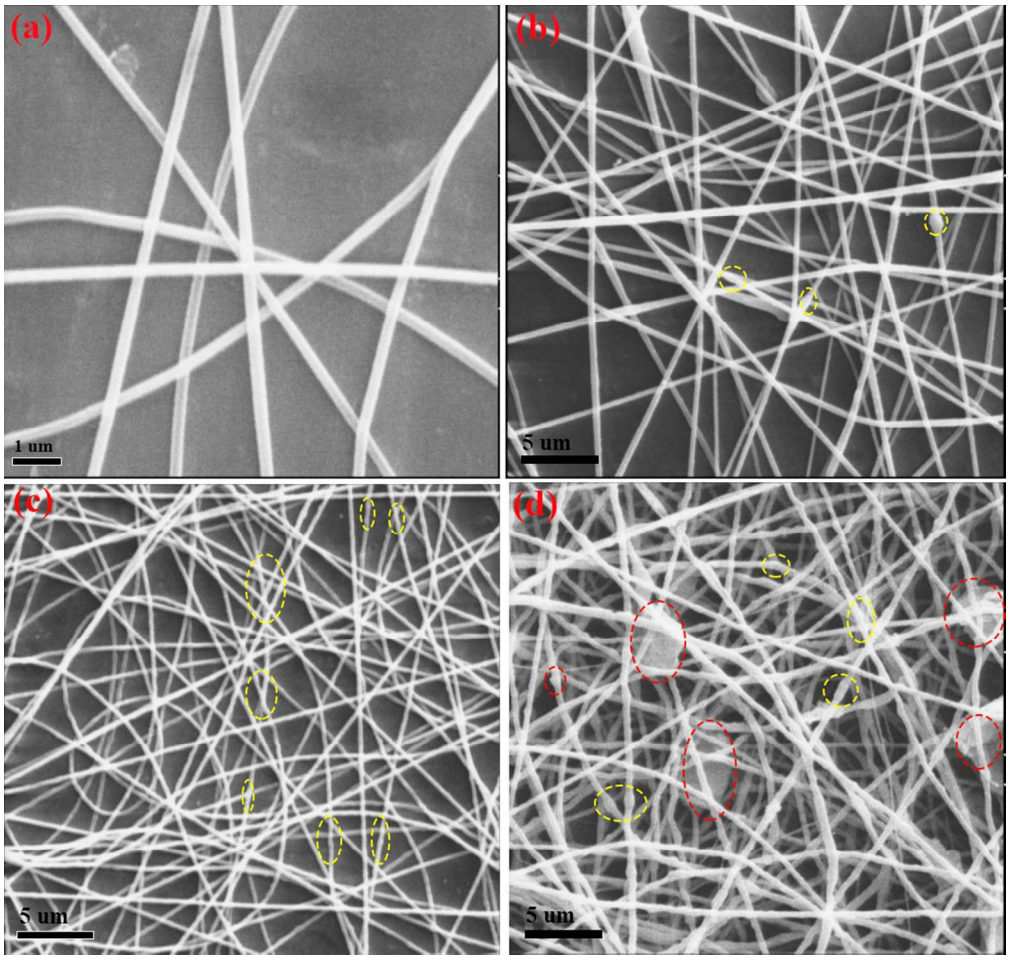

Figure 4. SEM images of PAA-PEO/Na-MMT nanocomposite fibes with 0.0 (a), 1.0 (b), 2.0 (c), and 4.0 wt.% Na-MMT (d)
383x363mm (72 x 72 DPI)

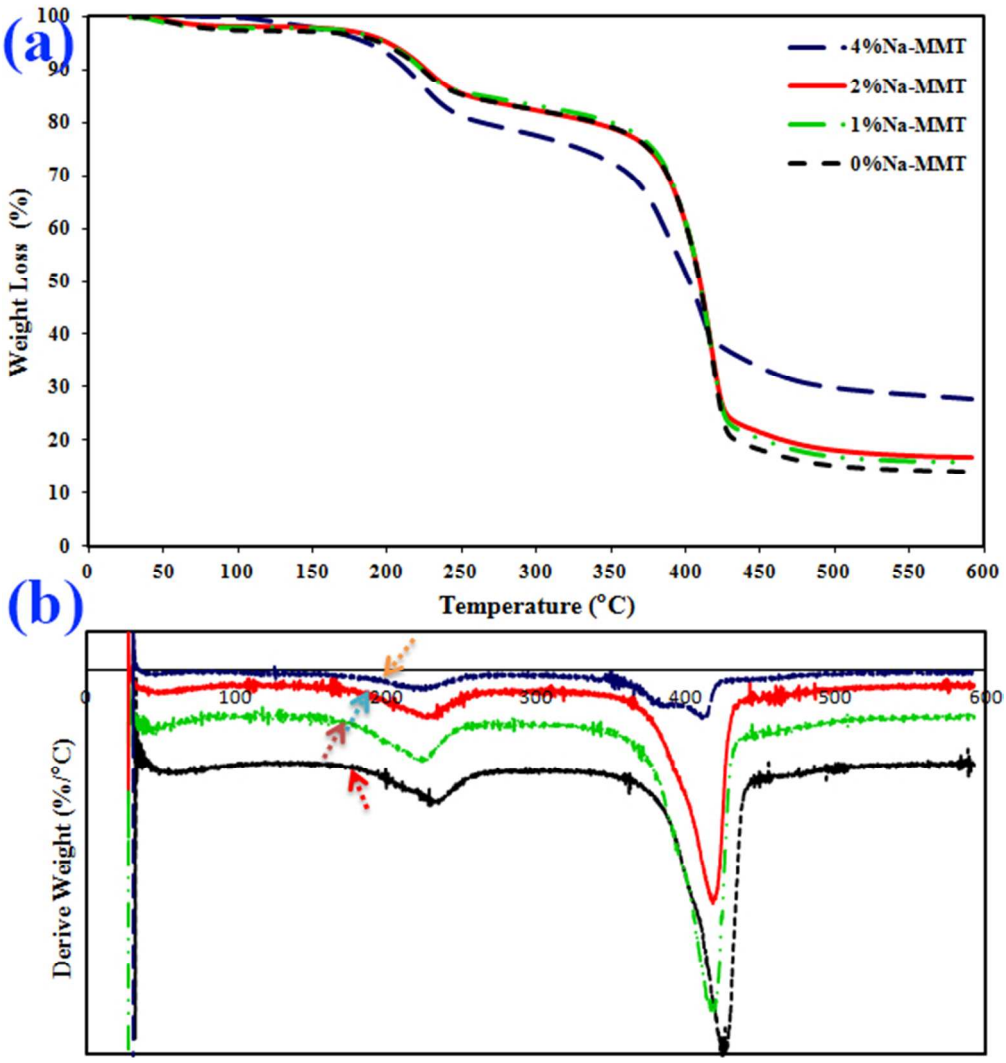

Figure 5. TGA (a) and DTGA (b) curves of pure PAA-PEO nanofibers and PAA-PEO/Na-MMT nanocomposite fibers
219x236mm (72 x 72 DPI)

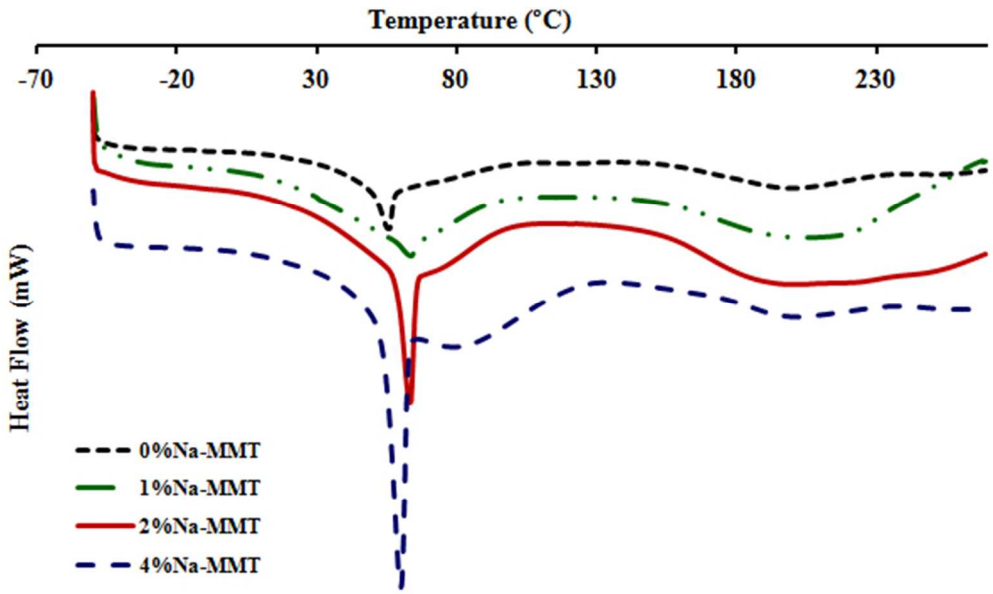

Figure 6. DSC curves of PAA-PEO nanofibers and PAA-PEO/Na-MMT nanocomposite fibers
157x93mm (96 x 96 DPI)

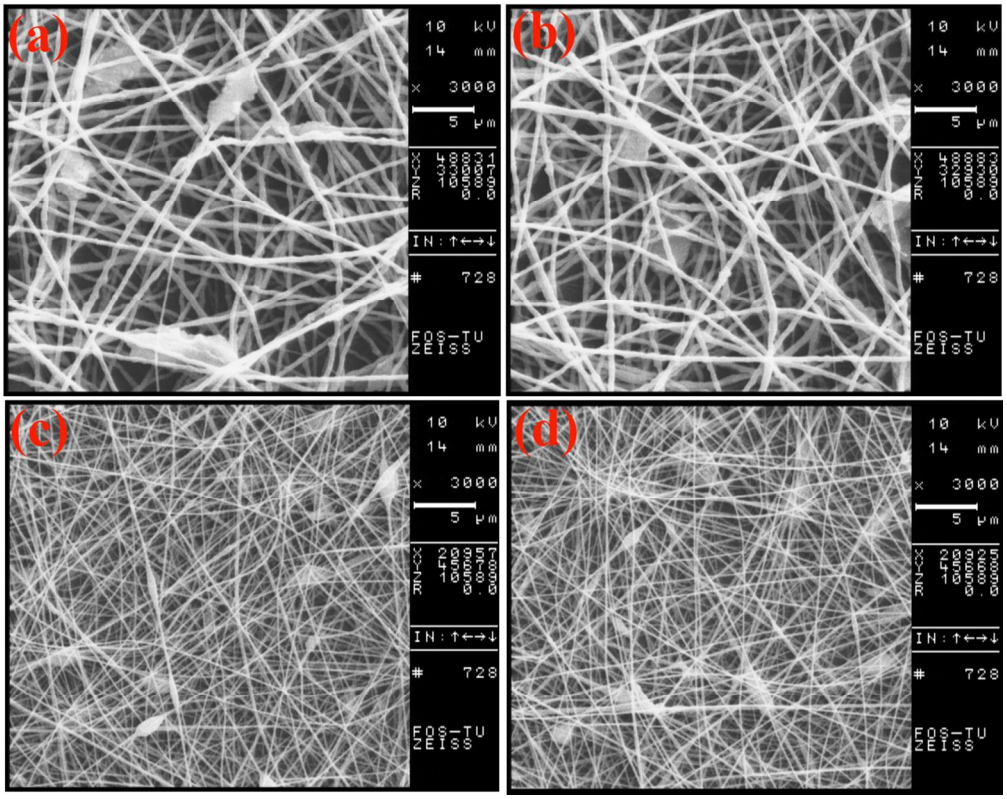

Figure 7. SEM images of electrospun PAA-PEO interpolymer complex containing 4.0 wt.% Na-montmorillonite in the various working distances: (a) 16.0 cm, (b) 17.5 cm, (c) 20 cm and (d) 22 cm
473x374mm (72 x 72 DPI)

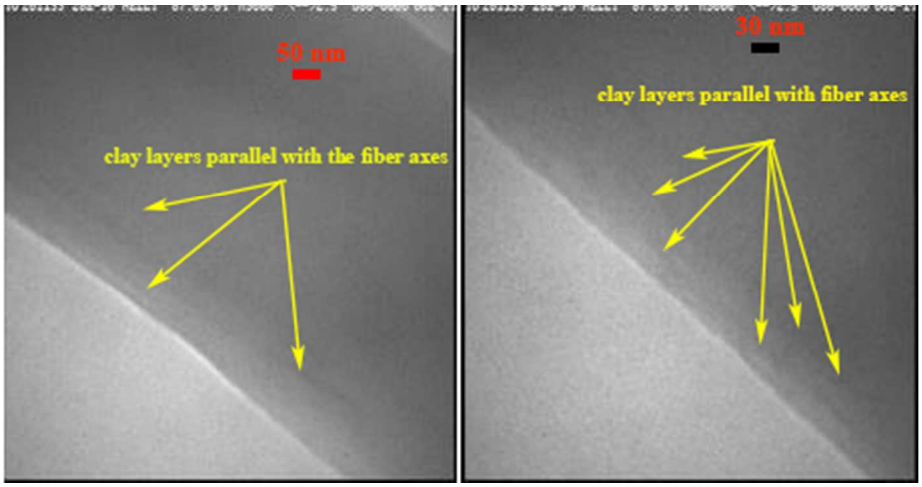

Figure 8. TEM images of electrospun PAA-PEO interpolymer complex containing 1.0 wt.% Na-montmorillonite
120x62mm (96 x 96 DPI)